

# An Extensible Induced Position Encoding Readout Method for Micropattern Gas Detectors

Shubin Liu, Siyuan Ma<sup>1D</sup>, Binxiang Qi, Zhongtao Shen, Guangyuan Yuan<sup>1D</sup>, and Qi An

**Abstract**—The large number of electronics channels has become an issue to the further applications of micropattern gas detectors (MPGDs) and poses a big challenge for the integration, power consumption, cooling, and cost. Induced position encoding readout technique provides an attractive way to significantly reduce the number of readout channels. In this paper, we present an extensible induced position encoding readout method for MPGDs. The method is demonstrated by the Eulerian path of the graph theory. A standard encoding rule is provided, and a general formula of encoding and decoding for  $n$  channels is derived. Under the premise of such method, a 1-D induced position encoding readout prototyping board is designed on a  $5 \times 5 \text{ cm}^2$  thick gas electron multiplier, where 47 anode strips are readout by 15 encoded multiplexing channels. Verification tests are carried out on an 8-keV Cu X-ray source with  $100\text{-}\mu\text{m}$  slit. The test results show a robust feasibility of the method and have a good spatial resolution and linearity in its position response. This method can dramatically reduce the number of readout channels, has potential to build large-area detectors, and can be easily adapted to other detectors like MPGDs.

**Index Terms**—Micropattern gas detector (MPGD), multiplexing readout, position encoding, tracking.

## I. INTRODUCTION

OVER the past 20 years, micropattern gas detectors (MPGDs) were widely used in high-energy physics, and had expanded to astrophysics, nuclear physics, and medical imaging.[1], [2] The conventional readout techniques employ a large number of electronic channels [3], which poses a big challenge to the further applications of MPGDs. By changing the readout electrodes' structure and multiplexing the readout channels, an induced position encoding technique for microchannel plate detector was developed by Kataria *et al.* [4] in 2007. This technique was used for MPGDs by Hu *et al.* [5] in 2011, where a preliminary feasibility test was implemented with Micromegas. This technique could significantly reduce the number of readout channels, but the foregoing works did not provide an extensible encoding method and the decoding was complicated. In this paper,

Manuscript received June 23, 2016; revised January 11, 2017, April 12, 2017, and May 18, 2017; accepted December 10, 2017. Date of publication December 13, 2017; date of current version February 13, 2018. This work was supported by the National Natural Science Foundation of China under Grant 11222552.

The authors are with the State Key Laboratory of Particle Detection and Electronics, University of Science and Technology of China, Hefei 230026, China (e-mail: liushb@ustc.edu.cn).

Color versions of one or more of the figures in this paper are available online at <http://ieeexplore.ieee.org>.

Digital Object Identifier 10.1109/TNS.2017.2782795

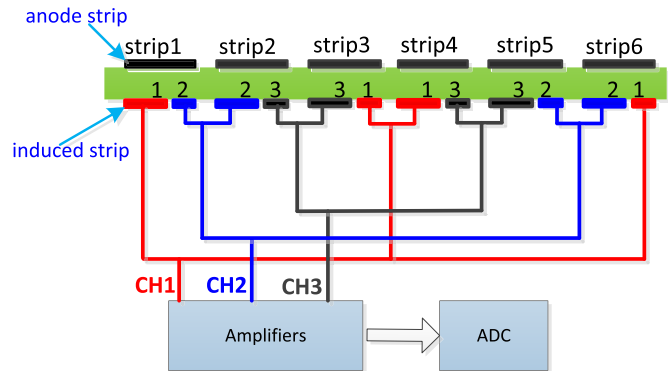


Fig. 1. Induced position encoding readout schematic.

TABLE I  
DECODING TABLE OF THREE READOUT CHANNELS

Channel: comparison	Strip: position
CH3>CH1	Strip 1
CH1>CH2	Strip 2
CH2>CH1	Strip 3
CH1>CH3	Strip 4
CH3>CH2	Strip 5
CH2>CH3	Strip 6

an extensible induced position encoding readout method for MPGDs is presented. This method is demonstrated by the Eulerian path of graph theory. A standard encoding rule is provided, and a general formula of encoding and decoding for  $n$  channels is derived. A prototyping design is implemented on a  $5 \times 5 \text{ cm}^2$  thick gas electron multiplier (THGEM), and verification tests are carried out on an 8-keV Cu X-ray source with  $100\text{-}\mu\text{m}$  slit.

## II. PRINCIPLE AND METHOD

### A. Principle

For ease of understanding, the simplified schematic is shown in Fig. 1, where six strips are readout by three encoded multiplexing channels. Charge from detectors is collected by an anode strip and split across two induced strips which correspond to the respective readout channels. Due to different widths, charge is split unequally between the two induced strips; thus, the amplitude on one is always higher than the other. Based on the signals' amplitudes in corresponding channels, the hit position could be uniquely decoded as shown in Table I.

TABLE II  
ENCODING LIST OF  $n$  READOUT CHANNELS

Row	Encoding list									
1	n1	12	21	13	31	...	1(n-2)	(n-2)1	1(n-1)	(n-1)1
2	n2	23	32	24	42	...	2(n-1)	(n-1)2	2n	
3	n3	34	43	35	53	...	3(n-1)	(n-1)3	3n	
...	...	...	...	...	...	...	...	...	...	...
k-1	nk	k(k+1)	...	...	k(n-1)	(n-1)k	kn			
...	...	...	...	...	...	...	...	...	...	...
n-1	n(n-1)	(n-1)n								

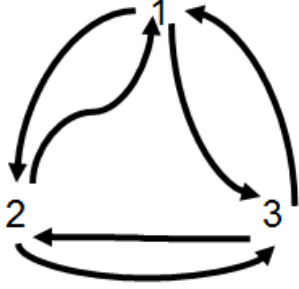


Fig. 2. Eulerian path.

### B. Eulerian Path Theorem

As shown in Figs. 1 and 3, readout channels have  $P_3^2$  ordered doublet combinations  $\{12, 23, 31, 13, 32, 21\}$  which correspond to six anode strips. This technique requires that any ordered doublet combination of channels appeared exactly once, and formed head to tail as an encoding list. Generally, the principle described above is a graph theory problem that whether there is an Eulerian path, where the doublet combinations represent the edges and the readout channels represent the vertices. Fig. 2 shows an Eulerian path of the three readout channels in Fig. 1. According to the Eulerian path theorem, it can be proved that there is an Eulerian path for  $n$  channels induced position encoding readout, as all of its vertices have an even degree. In other words,  $n$  channels can encode readout a maximum  $P_3^2$  anode strips.

### C. Encoding and Decoding

It turns out that there is more than one construction of Eulerian path. We need to make appropriate constraints to construct a regular and extensible encoding method so as to easily decode and design. As shown in Table II, it is an extensible encoding list for  $n$  channels, where the list is organized in rows. The encoding form  $XY$  means that the signal's amplitude of channel  $X$  is higher than channel  $Y$ .

According to Table II, the encoding formula (1) and decoding formula (2) can be derived as follows:

$$(xy)_i = \begin{cases} n, k & R = 1 \\ \left(k, \frac{R}{2} + k\right) & i = \text{even number} \\ \left(\frac{R-1}{2} + k, k\right) & i = \text{odd number} \end{cases}$$

$$R = i - (k-1)(2n-k) \quad (1)$$

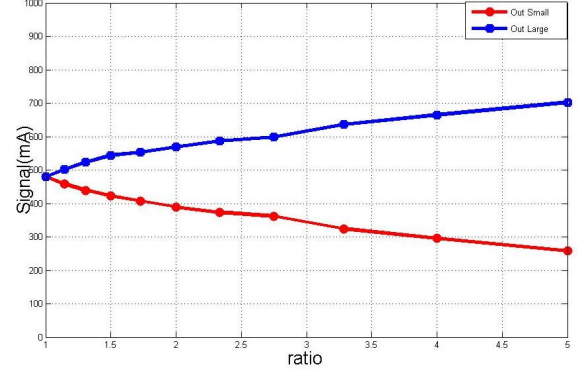


Fig. 3. Output signals of wide strip and narrow strip under different width ratios.

$$i_{(xy)} = \begin{cases} (y-1)(2n-y)+1 & ny \\ (y-1)(2n-y)+2(x-y)+1 & xy(x > y) \\ (x-1)(2n-x)+2(y-x) & xy(x < y). \end{cases} \quad (2)$$

### D. Optimize Width Ratio of Two Induced Strips

Every anode strip has two induced strips. One assumption of this method is that two adjacent induced strips get different induced charges, which means the width of two induced strips are different and the wider strip gets more charge. In order to optimize the width's ratio of the two induced strips, we did simulations with ANSYS's software designer and SIwave.

During the simulation, a fixed current of 1 mA flowed through the anode strip. By observing the current on the two induced strips, we could optimize the ratio of the two induced strips. In Fig. 3, we changed the width's ratio of the two induced strips and recorded the current on them.

It is necessary to ensure that not only the signals from the two induced strips have enough difference, but also the smaller signal can be distinguished easily from crosstalk and noise. So we did another simulation that when the two induced strips width's ratio was 2:1, the outputs of all the induced strips were recorded and drawn on Fig. 4. The input was a negative current pulse with amplitude of 1 mA on one anode strip. We could see that not only the two induced strips of the anode strip had signals, but also the adjacent induced strips had small pulses. In this condition when the ratio was 2, the largest signal had enough difference from the second largest signal. The second

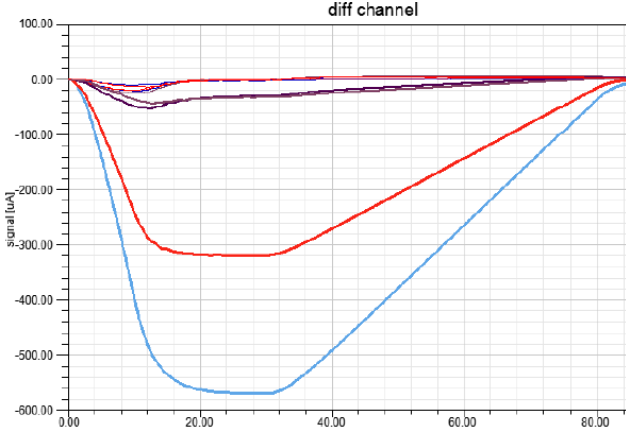


Fig. 4. Output signal of all electronic channels when ratio is 2:1.

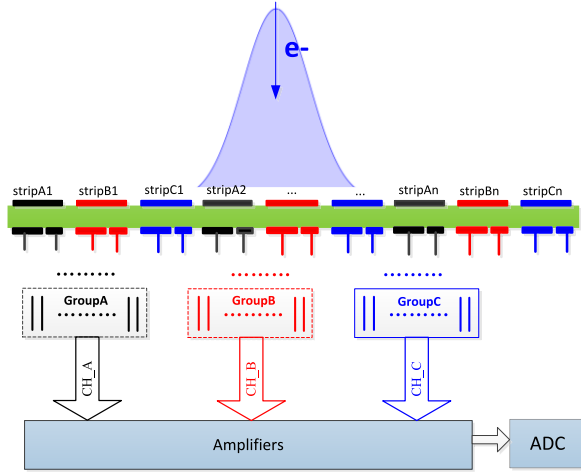


Fig. 5. Schematic of packet coding techniques.

largest signal could be distinguished easily from crosstalk and noise. As a result, we took 2 as the ratio of the two induced strips.

### E. Packet Coding Technique

The packet coding technique is proposed for the situation that signal has a certain width. If the width of input charge signal is narrower than the anode strip pitch, there is no need to use the packet coding technique. But, as shown in Fig. 5, in most cases, the input signal has a width larger than the anode strip pitch, which means the signal will hit more than one strip. Since the bases of this encoding method are the assumption that only one strip is hit, if the adjacent anode strips are hit at the same time, the decoded answer will have faults.

The packet coding technique is to separate adjacent strips into different groups in order to ensure that, in every group, no more than one strip is hit at the same time. The essence of groups A, B, and C in Fig. 5 is that each group encodes and decodes independently. By selecting the appropriate strip pitch and number of groups, the adjacent strips of the same group will not be hit when an event with a certain width comes.

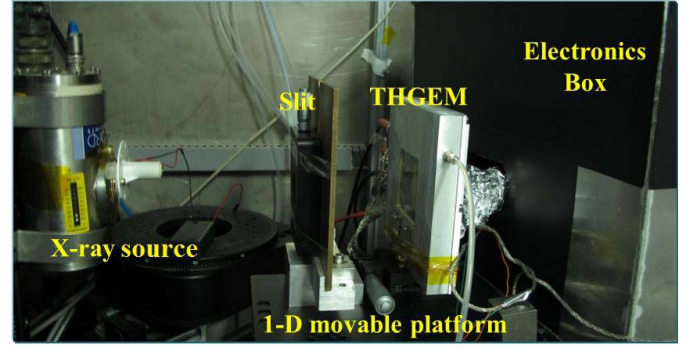


Fig. 6. Experimental setup.

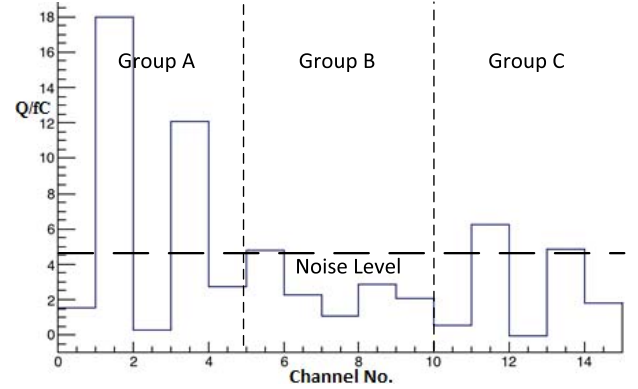


Fig. 7. Signal recorded on 15 channels when an event hit.

## III. VERIFICATION TEST

### A. Experiment for Verification

In order to verify this method, a prototyping readout board was manufactured and equipped for a  $5 \times 5 \text{ cm}^2$  THGEM detector [6]. To solve the case that each particle usually shows the signal on several neighboring strips, the neighboring strips are separated into three groups to encode, respectively. Based on the encoding list shown in Table II, the prototyping board has 47 1-D 1.07-mm strips which are readout by 15 channels. According to the decoding formula, the hit strip can be decoded by the fired channels.

As shown in Fig. 6, verification tests are carried out on the THGEM detector, which is filled with  $\text{Ar}/i\text{C}_4\text{H}_{10}$  (93:7) gas mixture. A  $100\text{-}\mu\text{m}$  slit in a thin brass sheet was used to produce a miniaturized X-ray beam. A manual movable platform was used for the position scanning test. The electronics are based on the VATA160 chip [7]

### B. Result of Tests

Fig. 7 shows the signals recorded on all 15 channels of one hit event. There are 47 anode strips, which are divided into three groups to be encoded and decoded individually, and the width of each strip is 1.07 mm. The baseline noise is about 2.5 fC. We take twice the noise of 5 fC as the noise threshold to filter the valid signals. It can be inferred that the hit channels are channel 2, channel 4, channel 12, and channel 14. Channel 2 and channel 4 belong to group A, from which the hit strip of strip 25 can be decoded. The channel 12 and channel 14 mean that strip 26 is hit, too.

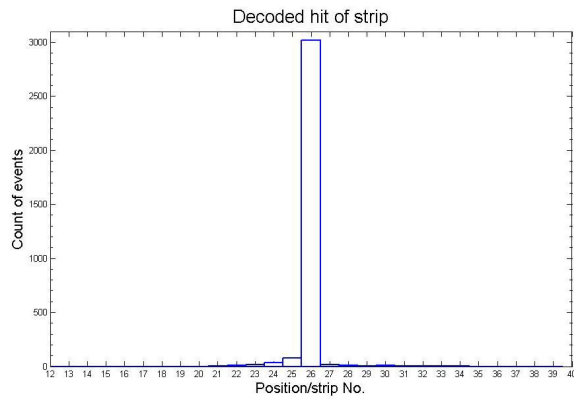


Fig. 8. Spatial resolution result of the detector.

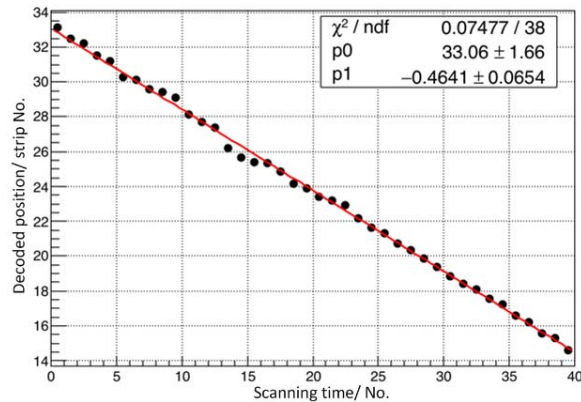


Fig. 9. Linear result of the position scanning test.

According to the distribution of charge on the two strips, the true hit point is strip 25.25, and the width of the event is about two strips, which means 2.14 mm.

Fig. 8 shows the decoded spatial resolution result of the detector. The width of anode strip is 1.07 mm. A large number of statistics have been made for a fixed X-ray incidence location. If the threshold is set to twice the noise, the correct rate of decoding can reach 94%. The root mean square (rms) of the statistical histogram is 1.69 strips, which mean the resolution is 1.8 mm.

Fig. 9 shows the results of linearity in the position scanning test. The test setup has been shown in Fig. 6. During the test, the detector was moved with a step of 0.5 mm every time.

The  $x$ -axis of Fig. 9 represents the number of the scanning, and  $y$ -axis means the decoded anode strip of each time. P1 shows the slope of the fit red line, which means that the step of every movement is 0.464 strips (0.496 mm). It is very close to the ideal step of 0.5 mm.

#### IV. CONCLUSION

A novel method of encoded multiplexing readout for MPGDs is presented in this paper. The method is demonstrated by the Eulerian path of graph theory. A standard rule for encoding is provided, and general formulas of encoding and decoding for  $n$  channels are derived. Under the premise of such rules, a 1-D position encoding readout circuit board is designed based on a  $5 \times 5$  cm<sup>2</sup> THGEM, and a verification test is carried out on an 8-keV Cu X-ray source with 100- $\mu$ m slit. The test results indicate that the method can decode the hit position. If the threshold is set to twice the noise, the correct rate of decoding can reach 94%. Concerning the correct rate of decoding, the rms of the position resolution is 1.69 strips, which means 1.808 mm. This method provides an attractive way to significantly reduce the number of readout channels. Inevitably, the method has some disadvantages, such as lowering the signal-to-noise ratio and lowering the detector's rate capability.

#### REFERENCES

- [1] M. Titov, "New developments and future perspectives of gaseous detectors," *Nucl. Instrum. Methods Phys. Res. A, Accel. Spectrom. Detect. Assoc. Equip.*, vol. 581, pp. 25–37, Oct. 2007.
- [2] Q. Liu *et al.*, "A successful application of thinner-THGEMs," in *Proc. 3rd Int. Conf. Micro Pattern Gaseous Detectors*, Zaragoza, Spain, Jul. 2013, paper 2013 JINST 8 C11008.
- [3] X. Ji, "PandaX-III: High-pressure gas TPC for Xe136 neutrinoless double beta decay at CJPL," *Bull. Amer. Phys. Soc.*, vol. 61, no. 6, Apr. 2016.
- [4] D. O. Kataria, R. Chaudery, and K. Rees, "High-speed position readout for microchannel plate-based space plasma instruments," *Nucl. Instrum. Methods Phys. Res. A, Accel. Spectrom. Detect. Assoc. Equip.*, vol. 573, pp. 240–242, Apr. 2007.
- [5] R. Hu *et al.*, "Preliminary test of one-dimensional position encoding read-out for MICROMEAS," *Nucl. Phys. Rev.*, vol. 28, no. 4, pp. 459–463, Apr. 2011.
- [6] H. B. Liu *et al.*, "A study of thinner-THGEM, with some applications," *J. Instrum.*, vol. 7, p. C06001, Jun. 2012.
- [7] C. Feng *et al.*, "Design of the readout electronics for the BGO calorimeter of DAMPE mission," *IEEE Trans. Nucl. Sci.*, vol. 62, no. 6, pp. 3117–3125, Dec. 2015.